Optical and Quantum Electronics (2020) 52:390
https://doi.org/10.1007/s11082-020-02512-4

Properties investigation of crystalline silicon surface irradiated by nanosecond laser pulses in different background atmospheres

Ji-Hong Zhao[1] · **Yang Yang**[1] · **Chao Li**[1]

Received: 18 March 2020 / Accepted: 13 August 2020 / Published online: 25 August 2020

Abstract
Black silicon materials were obtained by irradiation with ns laser pulses in different ambient atmospheres. The surface morphology, optical properties, and electrical properties of the black silicon were investigated after the ablation by ns laser pulses. Slab-like structures and boundaries were formed on the surface of black silicon fabricated in sulfur hexafluoride (SF_6), argon (Ar), and vacuum. In addition, a micrometer-sized sphere was observed at the tip of the slab-like structure, which was not obvious for the black silicon prepared in oxygen (O_2), nitrogen (N_2), and air. The infrared absorption of all the black silicon materials was enhanced. For the two samples fabricated in SF_6 and Ar, the infrared absorptance was approximately 50% at 1500 nm. A post-thermal annealing process decreased the infrared absorptance of all the black silicon materials except for that prepared in SF_6. The sheet resistance of the black silicon was reduced by the ns laser irradiation process, and thermal annealing further decreased the sheet resistance of all the samples except for the one fabricated in SF_6. After annealing at 875 K, the sheet carrier density of the black silicon fabricated in an Ar atmosphere and vacuum was approximately 10^{13} cm^{-2}, which was approximately three orders of magnitude larger than that of the silicon substrate (10^{10} cm^{-2}). The large difference in carrier density between the black silicon layer and substrate is beneficial for establishing contact junctions and for application in infrared photodetection.

Keywords Silicon · Nanosecond laser · Infrared absorption · Atmosphere

1 Introduction

Semiconductor silicon is the most commonly used semiconductor for discrete devices and integrated circuits. Silicon has impacted and is still greatly affecting modern civilization development (Iwai and Ohmi 2002). However, the energy bandgap and indirect band structure of crystalline silicon make it difficult to use silicon to produce some optical communication components such as lasers, LEDs, and photodetectors, seriously limiting its application in

✉ Ji-Hong Zhao
zhaojihong@jlu.edu.cn

[1] State Key Laboratory of Integrated Optoelectronics, College of Electronic Science and Engineering, Jilin University, 2699 Qianjin Street, Changchun 130012, China

silicon-based optoelectronic integration (Liu et al. 2007; Kasap 2001). To extend the absorption band of silicon to infrared wavebands, including the communication windows, textured silicon (black silicon) material fabricated by ultrafast laser pulses, such as femtosecond (fs), picosecond, and nanosecond (ns) laser pulses, has been widely investigated in recent years (Wu et al. 2001; Tull et al. 2009; Sardar et al. 2017; Crouch et al. 2004; Zorba et al. 2008), and this material has brought novel optoelectronic properties to semiconductor silicon, such as luminescence, infrared absorption, and an infrared detection ability (Wu et al. 2002; Chen et al. 2011; Zhao et al. 2015; Huang et al. 2006; Du et al. 2016). In comparison with the fs laser pulses, the ns laser pulses are prospective candidate for producing black silicon material since the ns-formed structures have a crystalline core and the surface is not disordered, in contrast to that of the fs-formed structures (Phillips et al. 2015). In addition, the ns laser has a lower use cost than the fs laser. According to previous studies, the black silicon obtained by ns laser pulses in an argon (Ar) atmosphere showed enhanced infrared absorption and excellent infrared photodetection ability, which was based on the rectification junction formed between the black silicon layer and silicon substrate (Li et al. 2018). Although no dopant was used, the resistivity of the silicon surface layer was reduced by approximately four orders of magnitude after ns laser irradiation; however, the reason for the change in resistivity is still not clear. Therefore, to further promote the infrared detection performance of black silicon, in this paper, the properties of black silicon irradiated by ns laser pulses in different atmospheres have been systematically researched and discussed.

2 Experiments

Crystalline silicon wafers were cleaned by a standard cleaning solution and then placed in a vacuum chamber, which was evacuated to 10 Pa (Li et al. 2018). Then, working gas at 1 atm was filled into the vacuum chamber if needed. In the laser irradiation experiment, a Q-switched Nd:YAG (neodymium-doped yttrium aluminum garnet) laser (Spectra Physics) was used to prepare black silicon materials. Here, the laser pulse duration and repetition rate were 10 ns and 10 Hz, respectively. To obtain a uniformly distributed laser beam, a frequency-tripled (wavelength of 355 nm) ns laser beam was expanded by an expansion system. Next, the laser beam was adjusted to an 8-mm diameter using a diaphragm and was then focused onto the silicon substrate surface by a 600-mm lens, and the diameter of the focused laser spot was approximately 180 μm. To achieve textured silicon samples with a large area, the substrate was moved along the S-line-scan route using a translation stage at a scanning speed of 250 μm s^{-1}.

After fabrication by the ns laser pulses, the surface morphology of the samples was obtained with a field emission–scanning electron microscope (SEM, JEOL JSM-7500F). Then, the optical properties of the samples were measured by a spectrophotometer (UV-3600) equipped with an integrating sphere (LISR-UV3100). Next, the electrical nature of the black silicon samples was analyzed by an ACCENT HL5500PC Hall system based on the van der Pauw method.

3 Results and discussion

In our experiments, crystalline silicon (111) substrates (n-type, thickness of 250 μm, $\rho > 4000\ \Omega$ cm) were irradiated by ns laser pulses in different ambient atmospheres, such as sulfur hexafluoride (SF_6), Ar, oxygen (O_2), nitrogen (N_2), air and vacuum. After irradiation

by ns laser pulses with a fluence of 7.88 J cm^{-2} above the ablation threshold, the surface of the crystalline silicon is melted and ablated by the ns laser pulse interaction; hence, the silicon surface is textured and modified. Figure 1a1–f1 show the surface morphology of black silicon samples fabricated in SF_6 ($\mathbf{S_S}$), Ar ($\mathbf{S_{Ar}}$), O_2 ($\mathbf{S_O}$), N_2 ($\mathbf{S_N}$), air ($\mathbf{S_{air}}$) and vacuum ($\mathbf{S_{vac}}$). Here, the label $\mathbf{S_i}$ represents the black silicon sample, and the subscript **i** indicates the atmosphere. For example, $\mathbf{S_S}$ and $\mathbf{S_O}$ indicate the black silicon samples obtained in SF_6 and O_2 atmospheres, respectively. Figure 1a2–f2 show local magnified images, which have a one-to-one correspondence with the images of Fig. 1a1–f1.

All these images, different as they seem, have one thing in common. For all the samples, radiated splashes can be observed clearly in the laser ablation regime, which is dependent on the heating effect from ns laser pulses. The surface morphology with radiated splashes is attributed to a linear absorption and thermal ablation process of ns laser pulses, which causes a large heat-affected zone that may induce melt re-deposition and shockwaves, leaving behind thermally induced radiated splashes (Sudani et al. 2009; Clark-MXR Inc. 2011). However, the radiated splashes and surface structures depend on the atmosphere used in which the ablation was carried out. For instance, for samples $\mathbf{S_S}$, $\mathbf{S_{Ar}}$, and $\mathbf{S_{vac}}$, slab-like structures and obvious boundaries induced by the partial overlap of the adjacent laser spots can be observed. Additionally, a smooth micrometer-sized sphere is clearly observed at the tip of the slab-like structure due to the melting process. Moreover, the structures on the sample $\mathbf{S_S}$ surface are sharper and thinner because of the chemical etching effect of SF_6 on silicon. In contrast, for samples $\mathbf{S_O}$, $\mathbf{S_N}$, and $\mathbf{S_{air}}$, the textured surfaces are rougher, and the boundaries of the slab-like structures are vaguer.

Afterward, the dependence of the optical properties of the black silicon samples on the different atmospheres was investigated. Figure 2a shows the reflectance (R) of the black silicon samples at wavelengths from 500 to 2500 nm. In comparison with the reflectance of the flat silicon substrate, for all the black silicon samples, the reflectance above the bandgap of silicon ($\lambda = 500$–1100 nm) is reduced by the ns laser irradiation. However, the reflectance of the black silicon samples depends on the atmosphere used. The reflectance of sample $\mathbf{S_{Ar}}$ is obviously lower than that of the silicon substrate, while it slightly varies for sample $\mathbf{S_S}$. The reduction of reflectance in this range ($\lambda = 500$–1100 nm) is related to the scattering effect of incident light on the textured silicon surface (Younkin et al. 2003). At the same time, the reflectance below the bandgap of silicon ($\lambda = 1100$–2500 nm) basically decreases for the majority of the black silicon samples after ns laser irradiation. Furthermore, within the range from 1100 to 2500 nm, the reflectance of sample $\mathbf{S_S}$ is the lowest, while that of sample $\mathbf{S_O}$ is the largest. The reduction of reflectance below the bandgap of silicon may be related to hyperdoping and structural defects induced by the ns laser ablation process (Barhdadi et al. 2011; Jackson et al. 1983).

Figure 2b shows the transmittance (T) of the black silicon samples and the silicon substrate. Compared to the transmittance of the silicon substrate, the transmittance above the bandgap of silicon ($\lambda = 250$–1100 nm) is almost unchanged for the black silicon samples. However, compared to that of the silicon substrate, the transmittance below the bandgap of silicon ($\lambda = 1100$–2500 nm) clearly decreases after irradiation with ns laser pulses for all the black silicon samples. Among them, the reduction of the transmittance is most obvious for samples $\mathbf{S_S}$ and $\mathbf{S_{Ar}}$.

Next, the absorptance (A) of the samples was calculated ($A = 1 - R - T$) and is shown in Fig. 2c. In comparison with the absorptance of the silicon substrate, the absorptance of all the black silicon samples is significantly enhanced by the laser ablation process in the range from 500 to 2500 nm. For the sample produced in an Ar atmosphere, the absorptance above the bandgap of silicon (500–1100 nm) is the largest and exceeds 95%. However, in

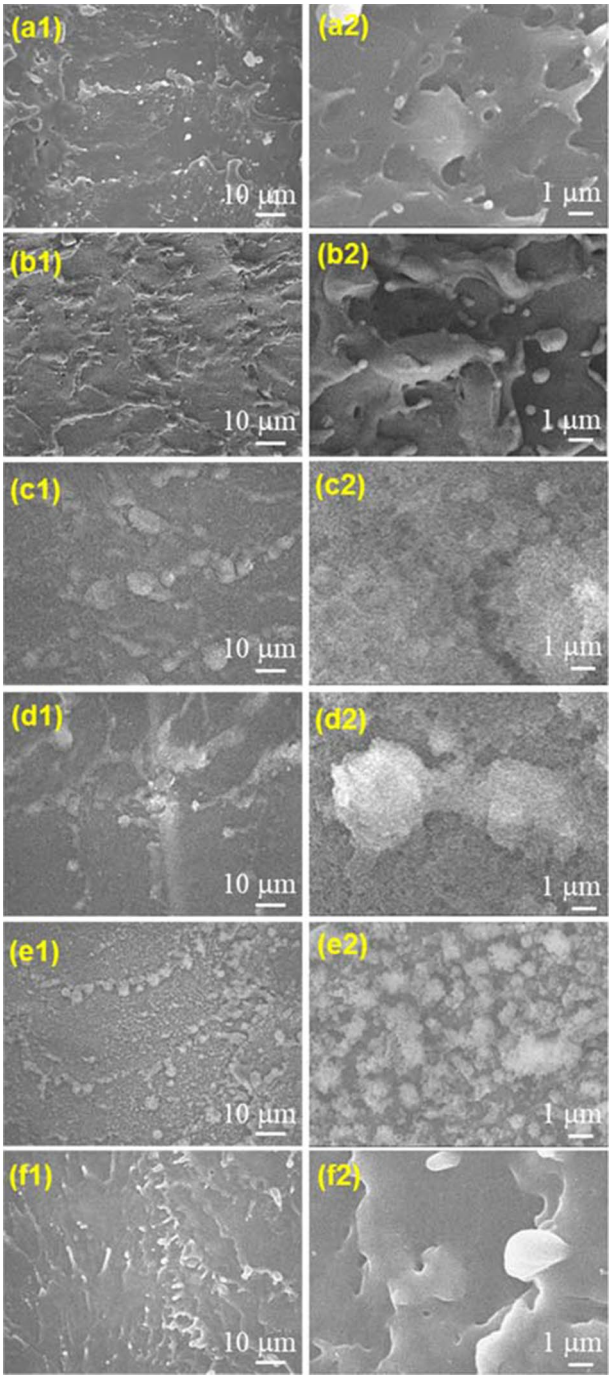

Fig. 1 **ai**–**fi** Show top-view SEM images of ns laser irradiated samples in ambient of **ai** SF_6, **bi** Ar, **ci** O_2, **di** N_2, **ei** air, and **fi** vacuum, respectively. i = 1, 2. **a2**–**f2** are the magnified images of (**a1**)–(**f1**)

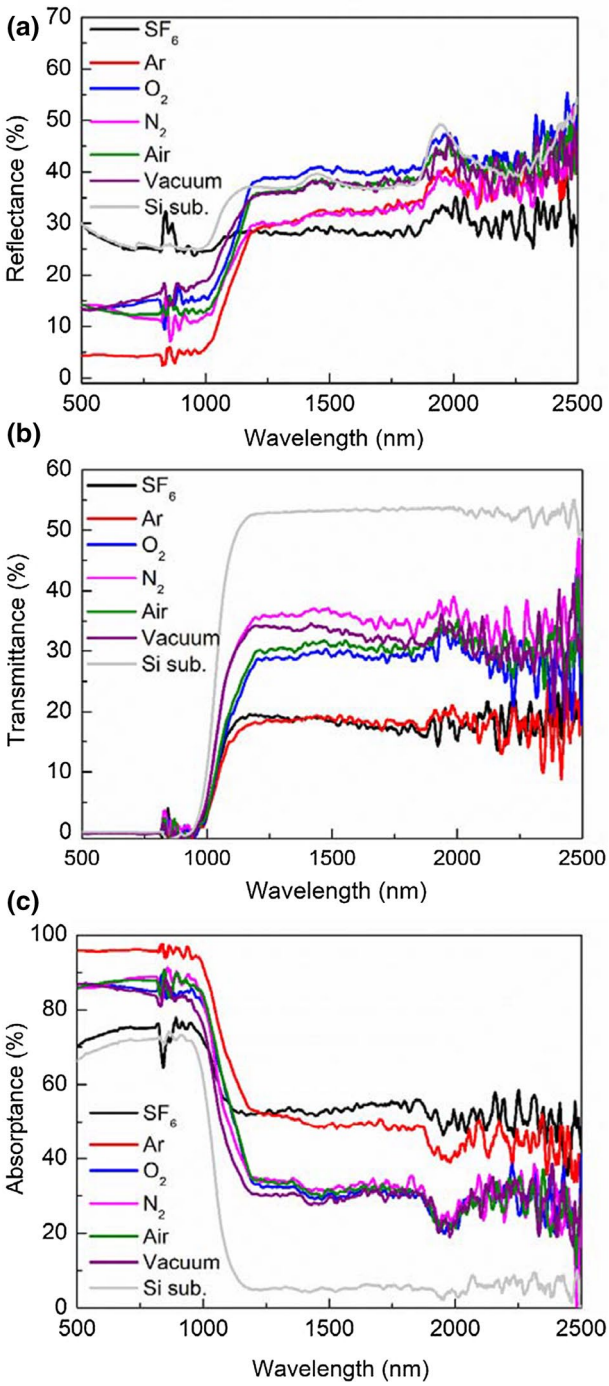

Fig. 2 **a** Reflectance of ns laser irradiated samples fabricated in ambient of different atmosphere; **b** Transmittance of ns laser irradiated samples; **c** The absorptance of ns laser irradiated samples

the wavelength range of 1100–2500 nm, the absorptance enhancement is the most notable for sample $\mathbf{S_S}$, followed by sample $\mathbf{S_{Ar}}$. Moreover, for samples $\mathbf{S_N}$, $\mathbf{S_O}$, and $\mathbf{S_{air}}$, their absorptances below the bandgap of silicon are very close to each other and slightly larger than that of the black silicon produced in vacuum. The absorption enhancement mechanism below the bandgap of silicon is very complex. For all the black silicon samples, the enhanced absorption should be related to the structural defects induced by ablation with the ns laser pulses (Barhdadi et al. 2011; Jackson et al. 1983). Among all the black silicon samples, sample $\mathbf{S_S}$ shows the largest enhancement in infrared absorption because the sulfur impurity levels (or band) and free carrier absorption can also contribute to the infrared absorption of sulfur-hyperdoped black silicon (Sher and Mazur 2014; Zhao et al. 2020).

Post-thermal annealing is a key step for improving the crystal quality of a black silicon layer and further producing a photodetector. To investigate the infrared absorption after thermal annealing, all the black silicon samples were thermally treated at 873 K for 30 min in a high purity Ar atmosphere (99.999%). The absorptance of the black silicon samples after annealing is shown in Fig. 3a. Compared to the absorptance of unannealed samples, the absorptance of the annealed black silicon is nearly unchanged in the range from 500 to 1100 nm, while it decreases in the range from 1100 to 2500 nm due to the thermal treatment. Post annealing, the infrared absorptance of black silicon $\mathbf{S_S}$ is still larger than that of the other black silicon samples. In addition, the infrared absorptances of black silicon $\mathbf{S_N}$, $\mathbf{S_O}$, and $\mathbf{S_{air}}$ tend to be the same and are slightly higher than that of black silicon $\mathbf{S_{vac}}$.

To give a quantitative variation in the infrared absorptance induced by the annealing process, $\mathbf{\Delta A}$ ($\Delta A = A_b - A_a$) is used for describing the variation in the absorptance. Here, A_b and A_a indicate the absorptance of black silicon samples before and after annealing, respectively. Figure 3b shows the variation in the absorptance (ΔA) for the different black silicon samples. From Fig. 3b, the infrared absorption is evidently reduced ($\Delta A \sim 20\%$) by the annealing process for black silicon $\mathbf{S_{Ar}}$. However, the variation in the infrared absorption is less than 10% for the other black silicon samples, which show a better thermal stability. To clearly observe the difference in the infrared absorption of samples before and after annealing, the absorptance at a wavelength of 1500 nm is further extracted and depicted in the insert in Fig. 3b. At 1500 nm, the absorptance is nearly unchanged for black silicon $\mathbf{S_S}$, while it is obviously reduced by the annealing process for black silicon $\mathbf{S_{Ar}}$. Furthermore, the variations in the absorptance at 1500 nm for black silicon $\mathbf{S_N}$, $\mathbf{S_O}$, $\mathbf{S_{air}}$, and $\mathbf{S_{vac}}$ are very similar to each other. From the above results, it can be considered that the infrared absorption related to the laser-induced structural defects can be reduced by the thermal annealing process, which means that the structural defects have a poor thermal stability. However, for black silicon $\mathbf{S_S}$, the very small change in the infrared absorption indicates that the absorption contributions related to sulfur impurity levels (or band) and free carriers, which are the main contributions to the infrared absorption of annealed black silicon $\mathbf{S_S}$, have a better thermal stability.

Afterwards, the electrical nature of the black silicon samples was investigated. Figure 4a shows that the sheet resistance (R_S) of the black silicon depends on the annealing temperature, which is in the range of 473–1023 K. After irradiation with ns laser pulses, the R_S values for all the samples are lower than that of the silicon substrate ($1.6 \times 10^5\ \Omega\ sq^{-1}$), and they are in the range of $(0.007–5.7) \times 10^4\ \Omega\ sq^{-1}$. The reduction in the sheet resistance is related to doping (for samples $\mathbf{S_N}$, $\mathbf{S_O}$, $\mathbf{S_S}$, and $\mathbf{S_{air}}$) or laser-induced structural defects (for all the samples). By comparison, owing to the hyperdoping of sulfur atoms, the sheet resistance decreases most obviously for sample $\mathbf{S_S}$, whereas there is little reduction in the sheet resistance for sample $\mathbf{S_N}$ due to the weak electro-activity of nitrogen impurities in silicon. After thermal annealing, the variation

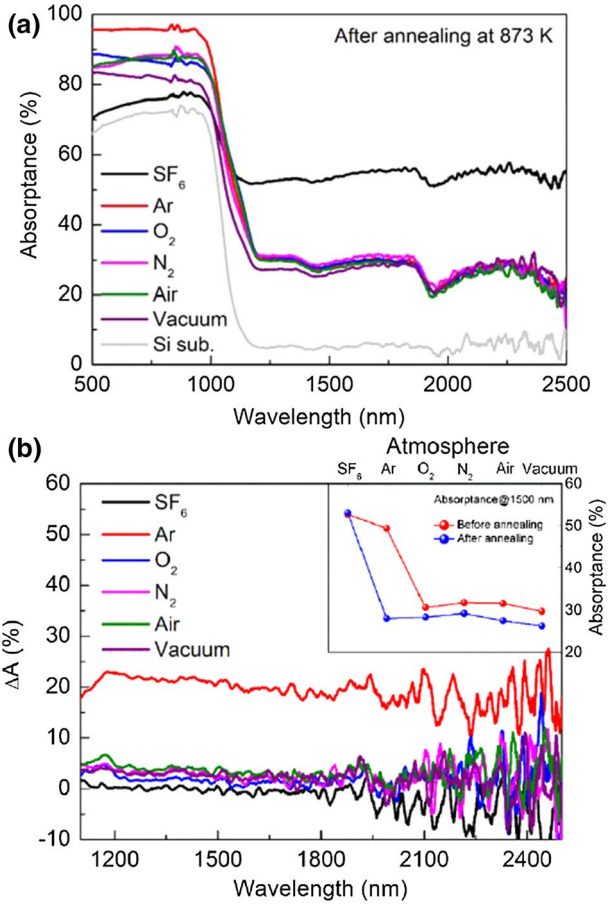

Fig. 3 **a** Absorptance of ns laser irradiated samples after thermal annealing at 873 K for 30 min; **b** the sub-bandgap absorptance variation of the black silicon samples. Insert is the absorptance of samples before and after annealing at wavelength of 1500 nm

in the sheet resistance is very small for black silicon $\mathbf{S_S}$. However, for the other black silicon samples, the sheet resistance decreases with increasing annealing temperature and is reduced by 1–2 orders of magnitude by annealing at 873 K. At a proper annealing temperature, the electrical activity of defect states can be optimally activated, such as 873 K for $\mathbf{S_{Ar}}$, $\mathbf{S_O}$, and $\mathbf{S_{vac}}$.

After annealing at 873 K, the carrier mobility and sheet carrier density of the black silicon samples were determined by Hall effect measurements and are shown in Fig. 4b. The sheet carrier density varies from 1.42×10^{13} (for $\mathbf{S_N}$) to 2.67×10^{14} cm^{-2} (for $\mathbf{S_S}$) for the black silicon samples obtained in different atmospheres, which shows a reverse trend to the sheet resistance in Fig. 4a because of the inversely proportional relationship between the sheet resistance and sheet carrier density. After laser irradiation, the carrier mobility of black silicon is lower than that of the silicon substrate and ranges from 262 to 382 $cm^2\ V^{-1}\ s^{-1}$. The lower carrier mobility is related to the textured rough surface and many defects in the black silicon layer. Moreover, owing to the strong scattering of ionized sulfur atoms, the mobility of the black silicon obtained in SF_6 is obviously lower than that of the other black silicon samples.

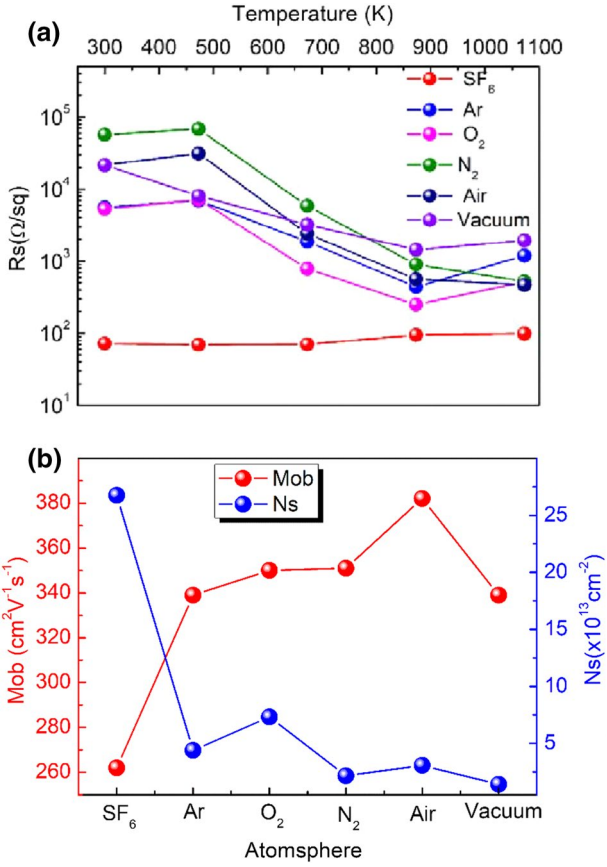

Fig. 4 **a** The resistance of the black silicon samples fabricated at atmosphere vs annealing temperatures. **b** Hall Effect measurements for sheet carrier density and carrier mobility of the black silicon samples fabricated at different atmosphere. All the samples are annealed at 873 K for 30 min

4 Conclusions

In conclusion, the surface modification of black silicon materials obtained under different ambient atmospheres has been investigated. First, the surface morphology of the samples is dependent on the ambient gas, and slab-like microstructures with a micrometer-sized sphere at the tip have been formed on the surfaces of samples $\mathbf{S_S}$, $\mathbf{S_{Ar}}$, and $\mathbf{S_{vac}}$, whose surfaces are smoother than those of the other three samples $\mathbf{S_O}$, $\mathbf{S_N}$, and $\mathbf{S_{air}}$. Second, the infrared absorption of all the samples is enhanced, and it increases most obviously for samples $\mathbf{S_S}$ and $\mathbf{S_{Ar}}$. After thermal annealing, the infrared absorption of sample $\mathbf{S_S}$ is still larger than that of the other samples. In addition, the infrared absorption is very similar for the other samples. Lastly, the sheet resistance is reduced by the irradiation with the ns laser pulses for all the black silicon samples, and it continues to be decreased by thermal annealing for all the samples except for sample $\mathbf{S_S}$. The difference in the carrier concentration between the black silicon layer and substrate is beneficial for establishing contact junctions, which can be applied for infrared photodetection. In sum, considering all the studied properties, such as a smoother surface, enhanced infrared absorption, and a larger difference in carrier concentration, the black silicon samples $\mathbf{S_S}$, $\mathbf{S_{Ar}}$, and $\mathbf{S_{vac}}$ are good choices for infrared photodetection applications.

Furthermore, $\mathbf{S_{Ar}}$ and $\mathbf{S_{vac}}$ are better for producing a photoconductive detector owing to their lower free carrier concentration.

Acknowledgements This work was supported by National Natural Science Foundation of China (NSFC) under Grants #61775077.

References

Barhdadi, A., Hartiti, B., Muller, J.C.: Active defects generated in silicon by laser doping process. Afr. Rev. Phys. **6**, 229–238 (2011)

Chen, T., Si, J., Hou, X., Kanehira, S., Miura, K., Hirao, K.: Luminescence of black silicon fabricated by high-repetition rate femtosecond laser pulses. J. Appl. Phys. **110**(7), 073106 (2011)

Clark-MXR Inc.: Machining with long pulse lasers (2011). http://www.cmxr.com/Education/Long.html. Accessed June 2019

Crouch, C.H., Carey, J.E., Warrender, J.M., Aziz, M.J., Mazur, E., Génin, F.Y.: Comparison of structure and properties of femtosecond and nanosecond laser-structured silicon. Appl. Phys. Lett. **84**(11), 1850–1852 (2004)

Du, L., Wu, Z., Li, R., Tang, F., Jiang, Y.: Near-infrared photoresponse of femtosecond-laser processed Se-doped silicon $n^+ - n$ photodiodes. Opt. Lett. **41**(21), 5031–5034 (2016)

Huang, Z., Carey, J.E., Liu, M., Guo, X., Mazur, E., Campbell, J.C.: Microstructured silicon photodetector. Appl. Phys. Lett. **89**(3), 033506 (2006)

Iwai, H., Ohmi, S.: Silicon integrated circuit technology from past to future. Microelectron. Reliab. **42**(4–5), 465–491 (2002)

Jackson, W.B., Johnson, N.M., Biegelsen, D.K.: Density of gap states of silicon grain boundaries determined by optical absorption. Appl. Phys. Lett. **43**(2), 195–197 (1983)

Kasap, S.O.: Optoelectronics and Photonics: Principles and Practices. Prentice-Hall, Upper Saddle River (2001)

Li, C.-H., Zhao, J.-H., Chen, Q.-D., Feng, J., Sun, H.-B.: Sub-bandgap photo-response of non-doped black-silicon fabricated by nanosecond laser irradiation. Opt. Lett. **43**(8), 1710–1713 (2018a)

Li, C.-H., Wang, X.-P., Zhao, J.-H., Zhang, D.-Z., Yu, X.-Y., Li, X.-B., Feng, J., Chen, Q.-D., Ruan, S.-P., Sun, H.-B.: Black silicon IR photodiode supersaturated with nitrogen by femtosecond laser irradiation. IEEE Sens. J. **18**(9), 3595–3601 (2018b)

Liu, J., Sun, X., Pan, D., Wang, X., Kimerling, L.C., Koch, T.L., Michel, J.: Tensile-strained, n-type Ge as a gain medium for monolithic laser integration on Si. Opt. Express **15**(18), 11272–11277 (2007)

Phillips, K.C., Gandhi, H.H., Mazur, E., Sundaram, S.K.: Ultrafast laser processing of materials: a review. Adv. Opt. Photon. **7**(4), 684–712 (2015)

Sardar, M., Chen, J., Ullah, Z., Jelani, M., Tabassum, A., Cheng, J., Sun, Y., Lu, J.: Multipulse nanosecond laser irradiation of silicon for the investigation of surface morphology and photoelectric properties. Mater. Res. Express **4**(12), 125902 (2017)

Sher, M.-J., Mazur, E.: Intermediate band conduction in femtosecond-laser hyperdoped silicon. Appl. Phys. Lett. **105**(3), 032103 (2014)

Sudani, N.: Thin wafer dicing using a high repetition rate femtosecond laser. Master's thesis, Ryerson University (2009)

Tull, B.R., Winkler, M.T., Mazur, E.: The role of diffusion in broadband infrared absorption in chalcogen-doped silicon. Appl. Phys. A **96**(2), 327–334 (2009)

Wu, C., Crouch, C.H., Zhao, L., Carey, J.E., Younkin, R., Levinson, J.A., Mazur, E., Farrell, R.M., Gothoskar, P., Karger, A.: Near-unity below-band-gap absorption by microstructured silicon. Appl. Phys. Lett. **78**(13), 1850–1852 (2001)

Wu, C., Crouch, C.H., Zhao, L., Mazur, E.: Visible luminescence from silicon surfaces microstructured in air. Appl. Phys. Lett. **81**(11), 1999–2001 (2002)

Younkin, R., Carey, J.E., Mazur, E., Levinson, J.A., Friend, C.M.: Infrared absorption by conical silicon microstructures made in a variety of background gases using femtosecond-laser pulses. J. Appl. Phys. **93**(5), 2626–2629 (2003)

Zhao, J.-H., Li, C.-H., Chen, Q.-D., Sun, H.-B.: Femtosecond laser direct writing assisted nonequilibriumly doped silicon n+-p photodiodes for light sensing. IEEE Sens. J. **15**(8), 4259–4263 (2015)

Zhao, J.-H., Li, X.-B., Chen, Q.-D., Chen, Z.-G., Sun, H.-B.: Ultrafast laser induced black silicon, from micro-nanostructuring, infrared absorption mechanism, to high performance detecting devices. Mater. Today Nano **11**, 100078 (2020)

Zorba, V., Boukos, N., Zergioti, I., Fotakis, C.: Ultraviolet femtosecond, picosecond and nanosecond laser microstructuring of silicon: structural and optical properties. Appl. Opt. **47**(11), 1846–1850 (2008)